ISSN: 0067-2904

Study the Adsorption of Basic Violet 10 Dye onto Olive Kernels Powder as Adsorbent in Aqueous Solution

Dunya Edan AL-Mammar, Rawaa Abbas Mohammed *
Department of Chemistry, College of Science, University of Baghdad, Baghdad, Iraq

Received: 5/1/2024 Accepted: 14/7/2024 Published: 30/6/2025

Abstract

The study evaluates the potential of powdered olive kernels as a natural adsorbent for extracting basic violet 10 dye from contaminated water using adsorption methods. The adsorbent material was characterized using Fourier transform infrared spectroscopy (FTIR) and atomic force microscopy (AFM). The impact of various operating variables namely, dosage of olive kernels powder, adsorption period, starting BV10 dye concentration, temperature and pH were investigated. The experimental data obtained from the equilibrium adsorption studies fitted better with the Freundlich adsorption isotherm model compared to the Langmuir isotherm model. Kinetics analysis for adsorption process revealed that the pseudo-second-order model (PSOM) was more appropriate to describe the sorption process constructed to pseudo-first-order (PFOM). Thermodynamics data for the adsorption of BV10 dye onto kernels powder surface display that this process is spontaneous and exothermic in nature.

Keywords: Biosorbent, Operating variables, Isotherm, Kinetics, Olive kernels.

دراسة امتزاز الصبغة القاعدية البنفسجية 10 على مسحوق نوى الزيتون كمادة مازة في المحاليل المائية

دنيا عيدان المعمار ، رواء عباس محمد *
قسم الكيمياء، كلية العلوم، جامعة بغداد، بغداد، العراق

الخلاصة

تقيم الدراسة امكانية مسحوق نوى الزيتون كمادة مازة طبيعية لاستخراج الصبغة القاعدية البنفسجية 10 من الماء الملوث باستخدام طرق الامتزاز. تم تشخيص المادة المازة باستخدام طيف الاشعة تحت الحمراء (FTIR) ومجهر القوة الذرية (AFM). تم دراسة تأثير المتغيرات التشغيلية المختلفة وهي، جرعة مسحوق نوى الزيتون، فترة الامتزاز، التركيز الابتدائي لصبغة BV10، درجة الحرارة والاس الهيدروجيني. النتائج التجريبية التي تم الحصول عليها من دراسات الامتزاز المتوازنة متوافقة بشكل افضل مع انموذج متساوي درجة حرارة الامتزاز فرندلش مقارنة بانموذج متساوي درجة حرارة الامتزاز لنكماير.

تحليل حركيات عملية الامتزاز يكشف ان إنموذج المرتبة الثانية الكاذبة (PSOM) اكثر ملائمة لوصف عملية الامتزاز بالمقارنة مع إنموذج المرتبة الاولى الكاذبة (PFOM). المعلمات الثرموديناميكية لعملية امتزاز الصبغة القاعدية البنفسجية 10 على سطح مسحوق نوى الزيتون يوضح ان العملية تلقائية وباعثة للحرارة بطبيعتها.

1. Introduction

Dyes are a major type of organic pollutants that contaminate water. They are widely used in industries such as textiles, plastics, paper, leather, and food processing [1]. The presence of low concentration of these compounds causes color interferes with a penetration of the sunlight into water and prevents photosynthesis [2, 3]. These substances are also carcinogenic for humans and cause bladder, liver, intestine and a skin cancer in human. Therefore, it is important to reduce the dye concentration in wastewater [4]. A treatment of dye effluents containing a toxic dyes represent a main technological challenge. Different methods are possible to discolorations such as ion-exchange, chemical precipitation, degradation and electrochemical destruction [5]. Adsorption has been considered as efficient, simple design and economically cheap process for removing the dye effluent from wastewater [6, 7]. Materials with high chemical stability, large surface area, and porous characteristics were preferentially selected as dye adsorbents due to these properties being conducive for effective adsorption [2]. Most investigation, has attracted a great interest in the using of a low-cost materials as adsorbents for treatments the wastewater [8], such as bagasse pith [9], periwinkle shell [10], coconut husk, sewage, wheat straw, perlite and agricultural waste [11]. These wastes materials have been applied as a cheap alternatives adsorbents for removal the color pollutants from wastewater [12, 13]. Olive oil wastes were used to remove heavy metal from aqueous medium [14, 15], also olive pomace was applied as alternative adsorbent for removal of disperse dyes [16], and nickel ions from water [17]. Recent investigations focused on the adsorption of BV10 dye onto biochar from olive biomass waste [18], modified olive stone activated carbon [18] and activated carbon derived from oil palm empty fruit bunches [19].

Basic violet 10 (BV10) is a xanthene-class dye that dissolves readily in water. It finds widespread application in coloring textiles, leather goods, printed paper, and various food products. This dye causes irritation to the skin, eyes and it have chronic toxicity and carcinogenic properties to humans and animals [20].

The purpose of this study is to investigate the adsorption potential of the olive kernels for uptake of BV10 dye from aqueous phase. Operational variables, isothermal, kinetics and thermodynamic studies controlling the sorption process were investigated.

2. Material and Methods

2.1. Adsorbent

Olive kernels (OK), which were used as the biosorbent, were collected and washed multiple times with warm distilled water to remove any soluble components. The washed olive kernels were then oven-dried at a temperature of 75°C for a duration of 48 hours. Then, the dried kernels are ground to a fine powder using mortar and pestle and finally dried at 100 ^{o}C. The dried powder was stored in a desiccator until it was used for the experiments.

2.2. Adsorbate

Basic violet 10 BV dye $C_{28}H_{31}ClN_2O_3$ supplied from Fluka, its molar mass 479.02 g.mol^{-1} and its IUPAC name [9-(2-carboxy phenyl)-6-diethyl amino 3 xanthenlidene]-diethyl ammonium chloride, C.I number 45170, solubility in water 15 gL^{-1} (20 ^{o}C), λ_{max} = 554 nm. Figure 1 shows the chemical structure for BV10 dye [21] .

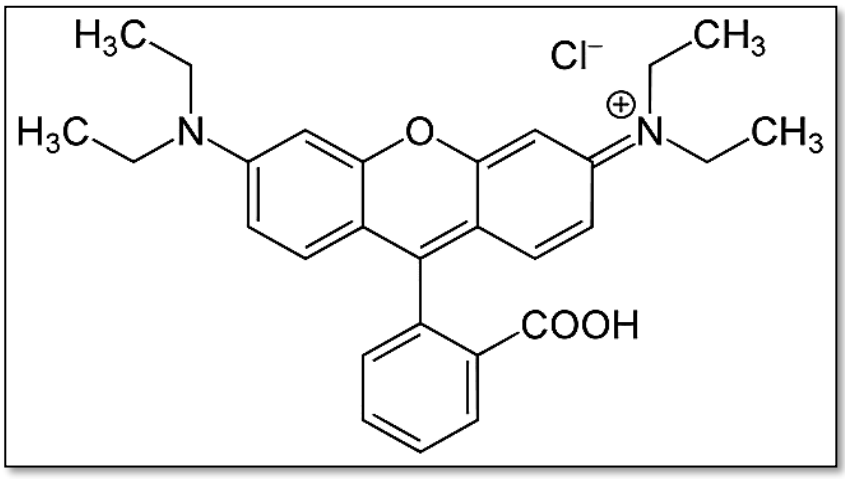

Figure 1: The Chemical structure for BV10 dye.

Double distilled water was used to prepare a stock solution of 1000 mg/L of BV10 dye by dissolving one gram of the pure dye in 1000 ml of double distilled water. The prepared solution was then used for further experiments by diluting it to the desired concentrations as required.

2.3. Characterization of the adsorbent

2.3.1. FT-IR analysis

This technique used to characterize the kernels olive as biosorbent and to identify the main functional groups that participate in the bonding between the dye species and adsorbent surface after adsorption. FTIR spectra were recorded using Shimadzu 3600-Japan over a wavelength range between 400 to 4000 cm^{-1}.

2.3.2. Atomic force microscopy (AFM)

AFM produces three-dimensional representations of surface topography at the granular level. Additionally, it offers precise measurements of a material's grain size [22]. AFM measurements performed using atomic force microscopy type (Naio AFM-2022 Switzerland).

2.4. Adsorption experiments

The adsorption experiments were conducted using a batch method. In this process, an accurately weighed amount of olive kernel was added to 25 ml of BV10 dye solution with a known concentration and pH. The mixture is stirred at 150 rpm for a choose adsorption period at constant temperature, then the supernatant was centrifuged for 5 min. The residual BV10 dye concentration was estimated by UV-Vis spectrophotometer type Shimadzu UV-1800 Japan at $\lambda_{max} = 554$ nm.

The following equations were used to determine the removal percentage R% for the dye and quantity of adsorbed dye q_e (mg/g) [23]:

$$R\% = \left[\frac{C_i - C_e}{C_i}\right] .100 \qquad ---------(1)$$

$$q_e = \frac{C_i - C_e}{W} (V) \qquad ----------(2)$$

Where C_i and C_e are the concentrations (mg/L) of the BV10 dye initially and at equilibrium, V is the volume of BV10 dye (L) and W is the mass of the olive kernel in (g).

The impact of several adsorption variables on the performance of the olive kernel powder as a biosorbent was investigated. These variables included: amount of olive kernels powder, adsorption period, initial BV10 concentration, temperature and pH.

The kinetics study were carried out using 0.2g as adsorbent dosage per 50ml from 15 mg/L BV10 dye concentration at pH equals to 7 and at 298K. 5ml were drawn from of the supernatant each 5, 10,20,30,40 min for the dye till reaching the equilibrium time. To separate liquid and solid phase, the suspension solutions were centrifuged for 5 minutes at 150 rpm. A clear supernatant was analyzed using UV-Vis spectrophotometer at λ_{max} 554 nm.

2.5. Adsorption isotherms

Two adsorption isotherms models were employed to describe the adsorption equilibrium data namely Langmuir and Freundlich adsorption isotherm, these models respectively written as the following equation [24]:

$$\frac{C_e}{q_e} = \frac{1}{K_L\, Q_m} + \frac{C_e}{Q_m} \qquad ----------(3)$$

$$\ln q_e = \ln k_{fr} + \frac{1}{n_f} \ln C_e \qquad ----------(4)$$

Where Q_m is the maximum mono layer coverage (mg/g), K_L is signifying Langmuir isotherm constant (L/mg), k_{fr} is a Freundlich isotherm constant (mg/g) $(L/mg)^{-1/n}$ and n_f is the intensity of adsorption.

The efficiency of adsorption was measured by separation factor R_s [24] :

$$R_s = \frac{1}{(1 + K_L C_i)} \qquad ----------(5)$$

Where C_i is the initial concentration $mg.L^{-1}$. The R_s values refer to the type of the adsorption: undesirable ($R_s > 1$), linear ($R_s = 1$), or irreversible ($R_s = 0$).

2.6. Adsorption kinetics

To describe the kinetics of BV10 adsorption on the kernels Olive powder, two kinetics models are applied pseudo-first-order (PFOM) and pseudo second order (PSOM). These models are respectively written based on the following equations [8, 25]:

$$\ln(q_e - q_t) = \ln q_e - k_1 t \qquad ----------(6)$$

$$\frac{t}{q_t} = \frac{1}{k_2 q_e^2} + \frac{t}{q_e} \qquad ----------(7)$$

Where k_1 (min^{-1}) and k_2 (g/mg.min), are PFOM rate constant and PSOM rate constant and q_t $(mg.\ g^{-1})$ is the amount of adsorbate at time t.

2.7. Thermodynamics study

To comprehend the spontaneous nature and ease of basic violet 10 dye adsorption onto powdered olive kernels (OK), it's necessary to analyze the thermodynamic parameters of the process. These parameters were tested at temperatures (293, 303, 313, and 323) K. The values of ΔH^o, ΔS^o, and ΔG^o were estimated by the following equations [26-28]:

$$\ln K_{eq} = \frac{\Delta S^o}{R} - \frac{\Delta H^o}{RT} \qquad ----------(8)$$

And

$$K_{eq} = \frac{q_e}{C_e} \qquad ----------(9)$$

Where R is the gas constant, T (K) is temperature. The values of ΔH^o and ΔS^o may be calculated from the slope and intercept of the Vant's-Hoff plot of $\ln K_{eq}$ vs. 1/T.

The values of ΔG^o were calculated by the following equation:

$$\Delta G^o = -RT ln K_{eq} \qquad ------(10)$$

3. Results and discussion:

3.1. Adsorbents characterization

3.1.1. Analysis of functional groups

FTIR spectra of olive kernels powder before after adsorption are shown in Figures (2 a, b). The material exhibited a broad absorption band from 3425.34 to 3382.91 cm-1, which is attributed to the O-H stretching vibration of alcohols and phenols as well as the N-H stretching vibration of amines [29], the absorption band at 2923.36 cm^{-1} and 2856.38 cm^{-1} refer to O-H carboxylic acid supported by C=O at 1652.88 cm^{-1}, and C-O at 1049.20 and 1031.85 cm^{-1}. The band at 1741.60 cm^{-1} relating to C=O of ester [30] bands at 1267.14 cm^{-1} and 1249.79 cm^{-1} corresponds to C-OH stretching. The FTIR analysis of the olive kernel powder before and after the adsorption of the dye, as shown in Figure 2b, revealed a shift in the band from 3425.34-3382.91 cm-1 to 3452.34-3369.41 cm-1 [31]. New peaks appeared at 819.69 cm^{-1} which related to aromatic vibrations and the bands at 1334.65-1323.08 cm^{-1} were linked to the stretching vibration of the C-N bond.

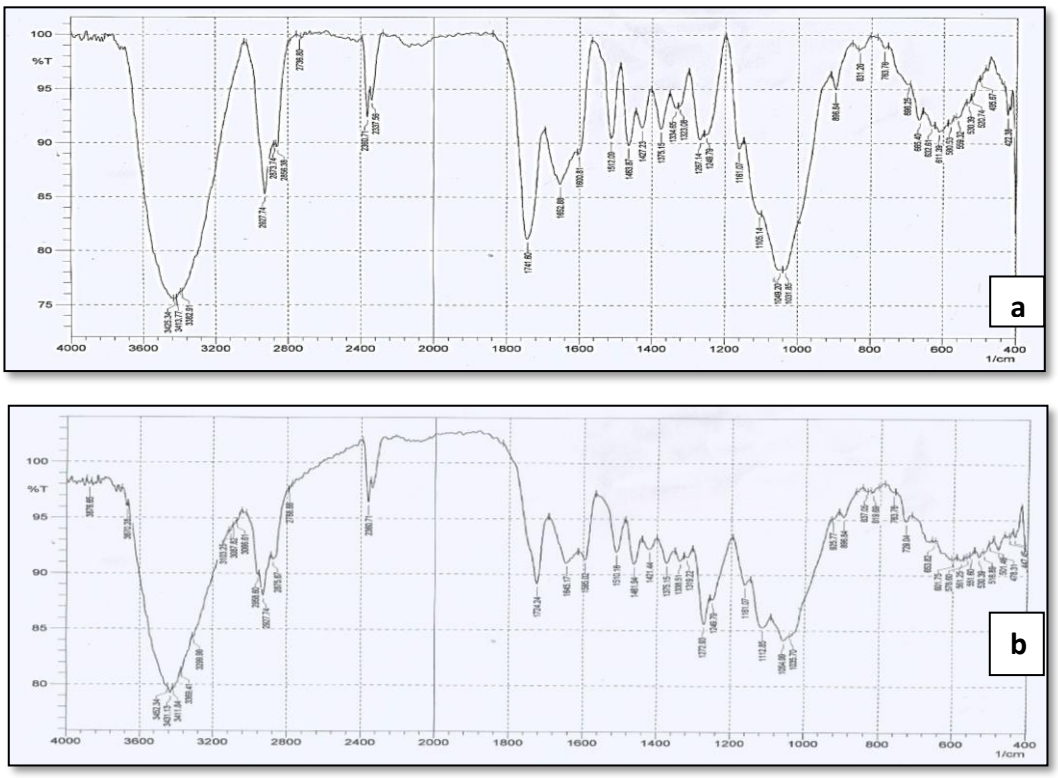

Figure 2: FTIR spectra for olive kernel powder, a- before adsorption, b- after adsorption.

3.1.2. Atomic force microscopy

This technique provides an information about the particles volume, average grains diameter and 3D pictures. Figures (3 a, b) point to a typical surface and the granularity cumulating distribution for the OK powder. The analyses revealed that the average observed diameter of the particles was 27.17 nm, while the average calculated volume was approximately 6.983 nm3.

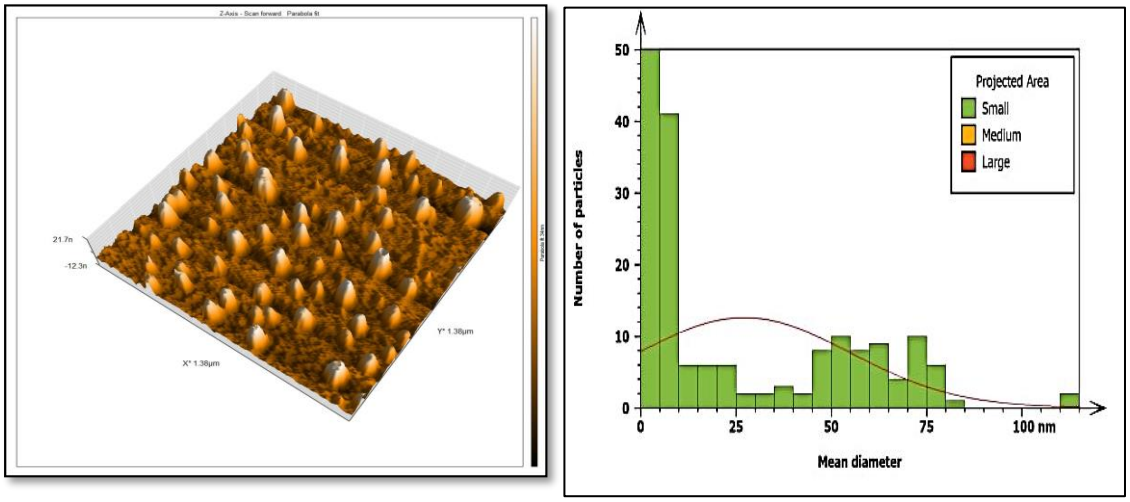

Figure 3: a-3D AFM image, b-Average mean diameter of OK sample.

3.2. Adsorption of BV10 dye onto olive kernels:

3.2.1. Spectrophotometric determined of BV10 dye

The absorption spectra of BV10 dye, Figure (4) were recorded using UV-Visible spectrophotometer at a wavelength 554 nm.

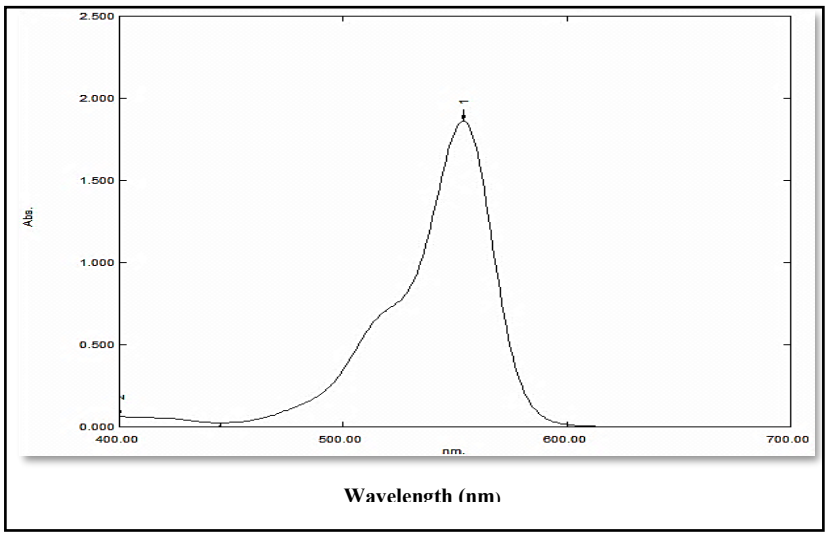

Figure 4: UV-Visible absorption spectrum of 10 mg/L BV10 dye.

3.2.2. Optimal operation variables for the adsorption of BV10 dye onto OK powder

3.2.2.1. Impact of OK powder dosage

The impact of OK powder dosage on the removal percentage of BV10 dye is established using various amounts of OK powder in the range (0.02 to 0.2 g) and 25 ml of 5mg/L dye solution at 298K, pH equals to 7, shaking speed 150 rpm and for one hour as adsorption time. The obtained results are shown in Figure (5). It is obvious from this Figure that the adsorption percentage increase from 37.8% to 73.5% with the increase of OK dosage from 0.02 to 0.1g, while between 0.1-0.2g OK dosage there is no obvious increase in the value of R%. The observed increase is attributed to the greater availability of adsorption sites on the surface of the olive kernel powder as the amount of adsorbent material is increased. Further increasing in the adsorbent amount did not show any increase in the removal percentage. This due to overlapping occurrence between the active sites at high amount of adsorbent [32].

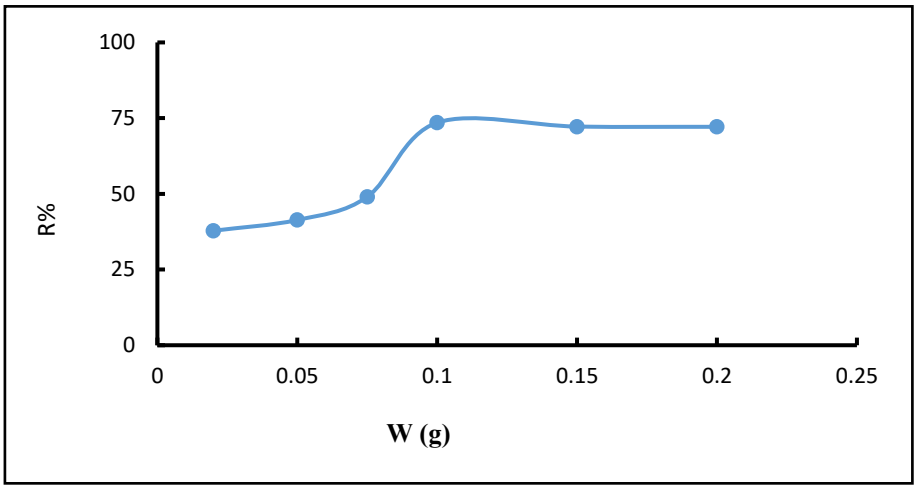

Figure 5: Impact of olive kernels powder dosage on the adsorption process.

3.2.2.2. Impact of adsorption period

The impact of adsorption period on the removal percentage of 5mg/L BV10 dye using OK powder as adsorbent is accomplished at a range of time 1-90 minutes, OK dosage 0.1g at 298K and pH 7. As evident from Figure 6, the removal percentage of the dye increased with increasing contact time between the olive kernel powder and the dye solution. The adsorption process reached equilibrium within 60 minutes, at which point the dye removal percentage reached 72.2%. After this equilibrium point, the removal rate remained almost constant. This may be attributed to availability of empty adsorption sites on the OK powder surfaces [33], and after one hour the vacant surfaces sites become saturated so the percentage of removal remains unchanged [34].

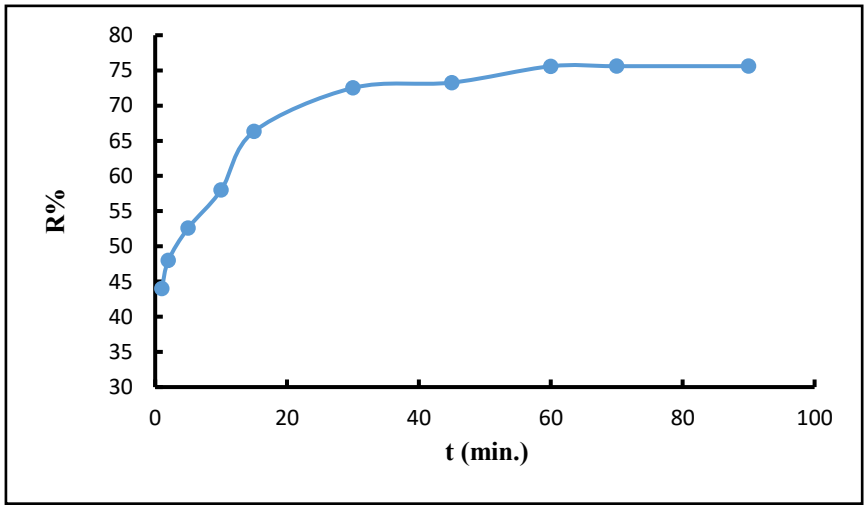

Figure 6: Impact of adsorption period on the adsorption of BV10 dye onto OK powder.

3.2.2.3. Impact of starting BV10 dye concentration

The effect of the initial BV10 dye concentration on the adsorption process was examined under the following conditions: dye concentrations were varied from 2-30 mg/L, olive kernel dosage was 0.1g, adsorption time was fixed at 1 hour, temperature was maintained at 293K and pH was set at 7. Under these parameters, the impact of changing the starting dye concentration was evaluated. It is evident from the Figure (7a), that when the starting BV10 concentration

increased from 2 to 30 mg/L the R% values change from 75% to 39.5%, this may be accounted to that: at low BV10 concentration, sufficient available active sites on OK surfaces are available, while increasing BV10 dye concentration leads to more occupation of the active sites, which making the sorption process limited. However, the actual amount of the adsorbed dye q_e is increased with increases BV10 dye concentration as shown in Figure (7b). This may be related to that at low starting BV10 dye concentration the ratio of number of available sites per unit dye concentration was small and adsorption become independent of the starting concentration, may be attributed to increased competition for the binding sites. While when the concentration of BV10 increases large number of the dye molecular were available per unit mass, appropriate the binding sites should be gradually filled up that leads to rising q_e values [35].

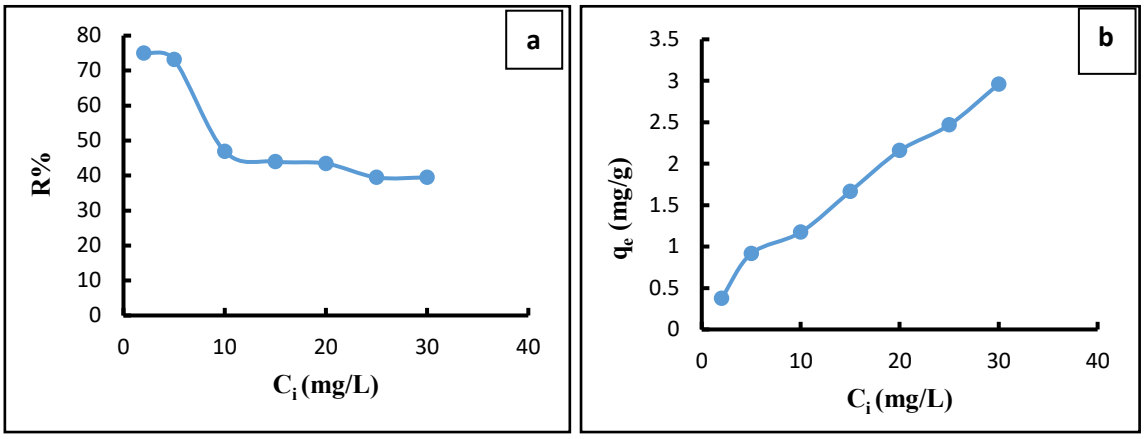

Figure 7:- Impact of starting BV10 dye concentration as a function of a-Removal percentage, b-The amount of BV10 adsorbed.

3.2.2.4. Impact of temperature

The effect of temperature on the removal percentage has been estimated at temperature range from 288 to 323K, BV10 concentration 5mg/L, keeping other operational conditions constant. The obtained results are represented in Figure (8). These results showed that values of R% decreased from 76% at 288 to 61.3% at 323K this may be reflected to the exothermic nature of the adsorption process [36].

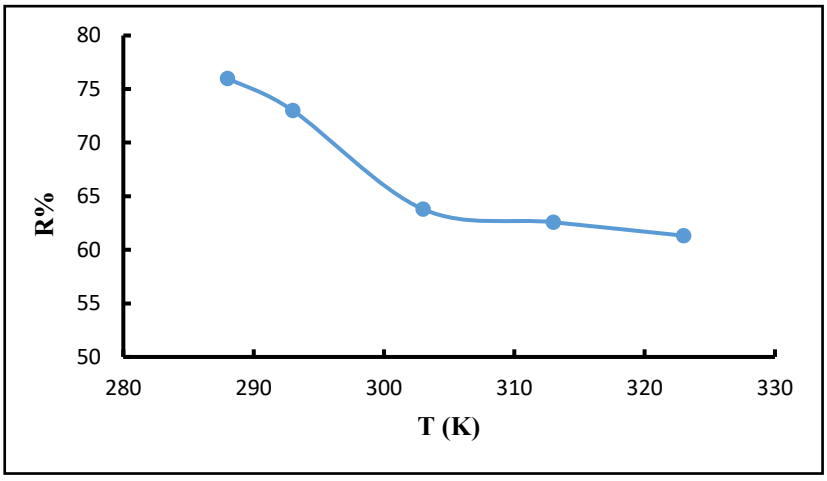

Figure 8:- Impact of temperature on the removal percentage for the adsorption of BV10 dye onto OK powder.

3.2.2.5. Impact of pH

The impact of pH on the BV10 removal using OK powder is tested in the pH range of 2.1 to 9 for 5mg/L dye concentration at 298K, with keeping other conditions constant. It is evident from Figure (9) that the percentage of removal for this dye increases from 40% at pH 2.1 to 67% at pH 9. It is found that the pH of the dye solution was 6.9. The pH of the solution influences both the electrical charge on the adsorbent surface and the ionic state of the dye molecules or other adsorbate. At low pH values BV10 dye as a cationic dye will compete with H^+ ions for adsorption sites of the OK surface that leads to decrease the R% values [37]. Conversely, at higher pH values, the adsorbents are negatively charged, so there is attractive force between the adsorbent and the dye that caused to improvement the adsorption process.

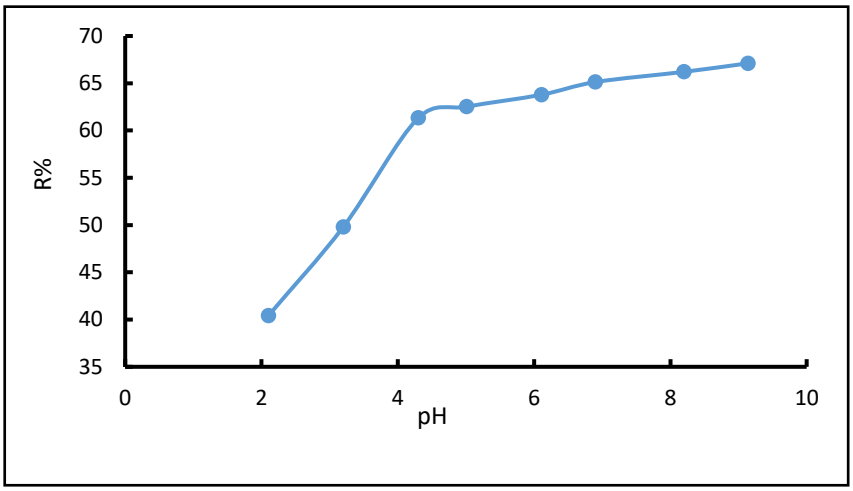

Figure 9: -Impact of solution pH on the removal efficiency of BV10 dye using OK powder.

3.3. Adsorption isotherms

Adsorption isotherms are illustrated by plotting the values of the amount of adsorbed dye qe (mg/g) versus the equilibrium concentration Ce (mg/L) at different temperatures. According to Giles classification [38, 39], the adsorption of BV10 dye onto OK powder follows L-type isotherm Figure (10). The type of adsorption isotherm observed in this study suggests that as the concentration of the solute (dye) in the solution increases, there is a gradual decrease in the available adsorption sites on the OK powder [40, 41].

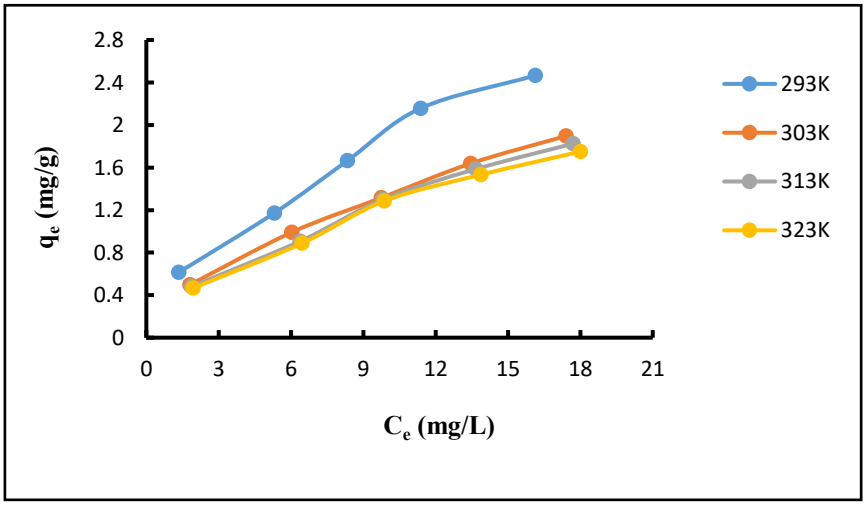

Figure 10: Adsorption isotherm for BV10 dye onto OK powder at different temperatures.

Figure (11 a,b) shows the plots of Langmuir and Freundlich isotherm for the adsorption of BV10 dye onto OK powder surface and isotherms data were presented in Table (1) as calculated from the intercepts and slopes of the plots. According to the values of R^2 for both types of isotherms the data best fitted with Freundlich isotherm with high correlation coefficient values. These values point to that the adsorption process was performed on heterogeneous surfaces [42]. However, the calculated R_s values that estimated from eq. (5) are $0< R_s <1$ revealed that the adsorption process is favorable. The values of $1/n_f$ where less than one indicates cooperative adsorption [43].Table (2) shows a comparison of previous maximum capacities of BV10 dye onto different adsorbents with the values obtained by using OK powder as adsorbent.

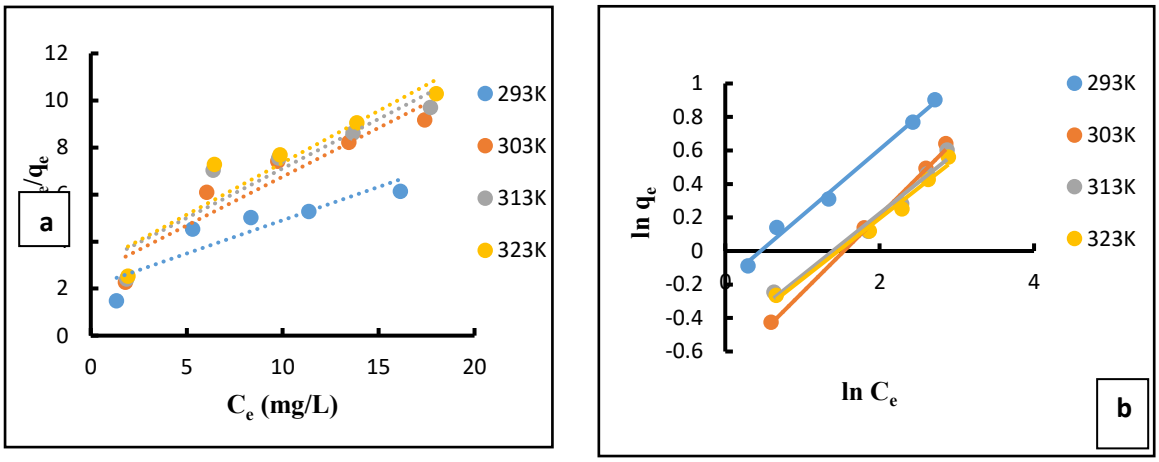

Figure 11:- Adsorption isotherm models plots a-Langmuir isotherm, b-Freundlich isotherm.

Table 1: Langmuir and Frundlich adsorption isotherm models constants.

Temp. (K)	Q_m	K_L	R^2	R_s (5 mg/L)	1/n	n	k_{fr}	R^2
293	3.5323	0.1363	0.8068	0.5946	0.3935	2.5429	0.8349	0.9922
303	2.4085	0.1593	0.8910	0.5566	0.4596	2.1758	0.4932	0.9913
313	2.3759	0.1453	0.8579	0.5792	0.3613	2.7078	0.5896	0.9860
323	2.2645	0.1504	0.8760	0.5706	0.3690	2.7100	0.5987	0.9785

Table 2: Comparison of the Q_m values of BV10 onto OK with different adsorbents.

Adsorbent	Q_m mg/g	Ref.
Modified muscovite clay	21.22	[8]
Raw dika nut	212.77	[44]
Acid-treated dika nut	232	[44]
Rhamnus stone	39.06-36.90	[29]
Modified coir pit	14.91	[45]
Activated asadiractalndica (neem) seed	90.91	[11]
Fly ash	10	[46]
Cedar cone	4.55	[31]
Oil-based drill cutting ash	50	[47]
Sugarcane baggs	51.5	[48]
Olive kernel powder	3.53 at 293K	This study

3.4. Adsorption kinetics

The kinetics of the adsorption of BV10 dye onto OK powder as adsorbent was tested using pseudo-first-order (PFOM) and pseudo second order (PSOM). Figure 12(a,b) displays the adsorption kinetic plots for PFOM and PSOM at 298K. The kinetic parameters estimated from fitting the PFOM and PSOM plots are presented in Table 3. This Table shows that k_1 value for BV10 dye was 0.0612 min^{-1}, k_2 was 0.3468 $g.mg^{-1}.min^{-1}$ and the R^2 values were 0.9745 and 0.9987 for PFOM and PSOM respectively. The calculated q_e cal. value for PFOM disagree with the experimental q_e exp., while for PSOM these values are almost agreed. This indicates that PSOM is better fit for the adsorption data than PFOM [49].

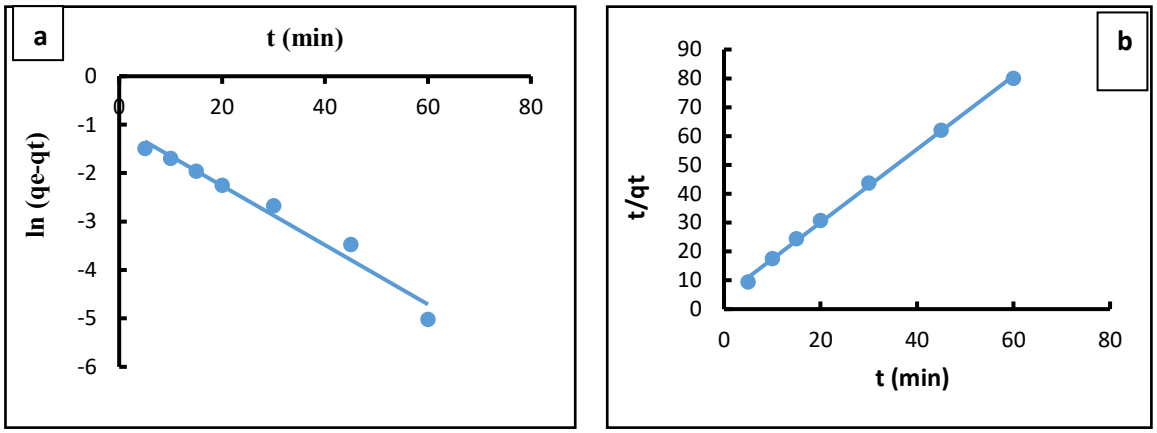

Figure 12:- Adsorption kinetics plots for a-PFOM, b-PSOM.

Table 3: -PFOM and PSOM kinetics data for the adsorption of BV10 dye onto OK powder.

C_i mg/L	Temp. (K)	PFOM				PSOM		
		$q_{exp.}$ mg/g	q_e cal mg.g^{-1}	k_1 1/min	R^2	q_e cal mg/g	k_2 g/mg.min	R^2
10	298	0.7566	0.3542	0.0612	0.9715	0.7874	0.3468	0.9987

3.5. Thermodynamic study:

Thermodynamic data estimated for the adsorption of BV10 dye onto OK powder are reported in Table (4). The values of ΔS^o, ΔH^o were predicted from the intercept and slope of the Vant-Hoff plot Figure (13), while the values of ΔG^o can be calculated directly from eq. (9). As shown in Table (4) it was found that the values of ΔG^o is negative at given temperature which donates that the adsorption process is favorable and spontaneous [50, 51], in addition, these values decreases with increase the temperature, that shows the mobility of BV10 dye molecules at the higher temperature. However the less values of ΔH^o (<40 kJ/mol) predicted that the adsorption process is phsi-sorption type. The negative ΔH^o values confirms that the adsorption process is exothermic in nature, and the negative values of ΔS^o demonstrate a decrease in the randomness that appears at the solid/solution interface among the sorption process [52].

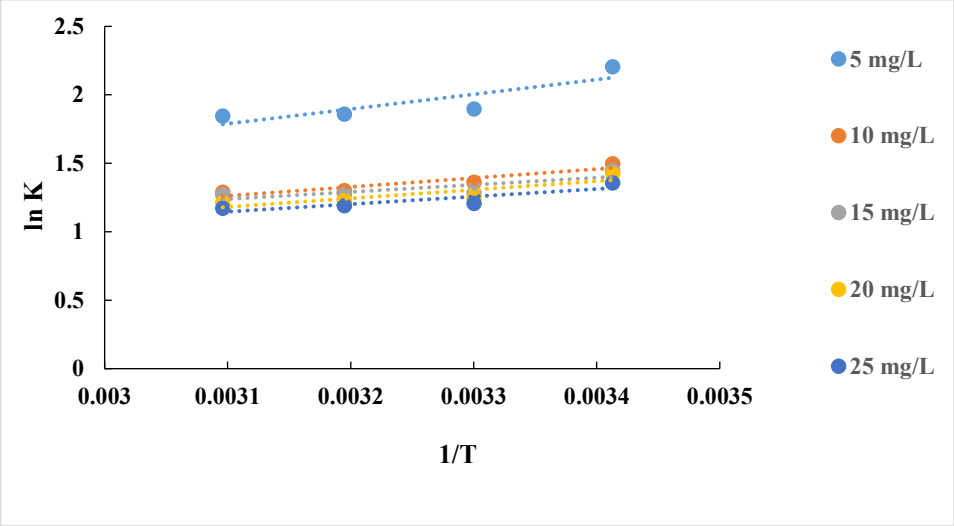

Figure 13:- Thermodynamic data for the adsorption of BV10 dye onto OK powder surface.

Table 4:- Thermodynamic data for the adsorption of BV10 dye onto OK powder.

C_1 mg/L	-ΔH° kJ/mol	-ΔS° J/mol	-ΔG° kJ/mol			
			293K	303K	313K	323K
5	8.9290	12.8077	5.1763	5.0483	4.9202	4.7921
10	5.4130	6.2862	3.5713	3.5085	3.4455	3.3826
15	4.3380	3.1501	3.4148	3.3834	3.3519	3.3204
20	5.2178	6.3550	3.3558	3.2922	3.2287	3.1658
25	4.5949	4.7115	3.2144	3.1673	3.1202	3.0731

Conclusions

This research investigated the use of powdered olive kernels as an adsorbent to eliminate basic violet 10 dye from contaminated water. The maximum dye removal was noticed 73.5% at 0.1g adsorbent dosage and 75% for 2mg/L starting dye concentration, 72.2% for one hour as an adsorption period and 67% at pH 9. The values of R% decrease from 76% to 61.3% when the temperature increase from 288K to 323K. According to Giles classification for the adsorption isotherms, the adsorption of BV10 dye onto OK powder follows L-type. In addition, Freundlich isotherm model describe the adsorption process better than Lungmuir isotherm model. The kinetic studies were best described by the pseudo-second-order model. The obtained thermodynamic data such as ΔH^o, ΔG^o and ΔS^o demonstrated that the adsorption process was exothermic, spontaneous occurs with decrease in randomness at the solid/solution interface. The findings of this research demonstrate that olive kernels serve as an efficient and environmentally friendly adsorbent material for extracting BV 10 dye from water-based solutions.

References

[1] H. Tahir, M. Sultan, and Q. Jahanzeb, "Remediation of azo dyes by using household used black tea as an adsorbent," *African Journal of Biotechnology,* vol. 8, 2009.

[2] Z. Shahryari, A. S. Goharrizi, and M. Azadi, "Experimental study of methylene blue adsorption from aqueous solutions onto carbon nano tubes," *International Journal of water Resources and environmental engineering,* vol. 2, pp. 016-028, 2010.

[3] A. Q. Khanjar, A. M. Farhan, and A. M. Rheima, "The Adsorption Ability of Cibacron Red Dye from Aqueous Solution Using Copper Oxide Nanoparticles," *Baghdad Science Journal,* vol. 21(6), pp. 1994-2006, 2024.
[4] Y. Zheng, B. Zhu, H. Chen, W. You, C. Jiang, and J. Yu, "Hierarchical flower-like nickel (II) oxide microspheres with high adsorption capacity of Congo red in water," *Journal of colloid and interface science,* vol. 504, pp. 688-696, 2017.
[5] I.-M. Boukerzaza, B. Boulhouchet, B. Kebabi, and A. Mennour, "Adsorption Of Rhodamine B Onto Olive Pomace: Isotherms, Kinetics And Infrared Studies," *Environmental Engineering & Management Journal (EEMJ),* vol. 20, 2021.
[6] Y. Kuang, X. Zhang, and S. Zhou, "Adsorption of methylene blue in water onto activated carbon by surfactant modification," *Water,* vol. 12, p. 587, 2020.
[7] R. L. Khalaf, I. M. Almousawi, and A. M. Rheima, "Dye pollution removal in aqueous solution using novel photochemically synthesized CoZnFe2O5 nanocomposite," *Desalination And Water Treatment,* vol. 243, pp. 287-293, 2021.
[8] M. N. Rashed, A.-S. A. G. Arfeen, and F. A. El-Dowy, "Removal Of Rhodamine-B Dye Using Chemically Modified Activated Muscovite: Kinetics, Isotherms, And Thermodynamic Studies," *Journal of Chemical Technology & Metallurgy,* vol. 58, 2023.
[9] H. M. Gad and A. A. El-Sayed, "Activated carbon from agricultural by-products for the removal of Rhodamine-B from aqueous solution," *Journal of Hazardous Materials,* vol. 168, pp. 1070-1081, 2009.
[10] O. S. Bello and M. A. Ahmad, "Removal of Remazol Brilliant Violet-5R dye using periwinkle shells," *Chemistry and Ecology,* vol. 27, pp. 481-492, 2011.
[11] E. Porselvi and P. Krishnamoorthy, "Adsorptive Removal of Rhodamine-B by Agricultural Waste," *Oriental Journal of Chemistry,* vol. 29, p. 719, 2013.
[12] H. H. Kadhim and K. A. Saleh, "Removing Cobalt ions from Industrial Wastewater Using Chitosan," *Iraqi Journal of Science,* vol. 63, pp. 3251-3263, 2022.
[13] N. H. AL-Shammari and D. E. AL-Mammar, "Adsorption of Biebrich Scarlet Dye into Remains Chromium and Vegetable Tanned Leather as Adsorbents," *Iraqi Journal of Science,* vol. 63, pp. 2814-2826, 2022.
[14] M. Martín-Lara, F. Hernáinz, M. Calero, G. Blázquez, and G. Tenorio, "Surface chemistry evaluation of some solid wastes from olive-oil industry used for lead removal from aqueous solutions," *Biochemical Engineering Journal,* vol. 44, pp. 151-159, 2009.
[15] A. M. Farhan, A. M. Zaghair, and H. I. Abdullah, "Adsorption Study of Rhodamine–B Dye on Plant (Citrus Leaves)," *Baghdad Science Journal,* vol. 19, pp. 0838-0838, 2022.
[16] V. Rizzi, F. D'agostino, P. Fini, P. Semeraro, and P. Cosma, "An interesting environmental friendly cleanup: The excellent potential of olive pomace for disperse blue adsorption/desorption from wastewater," *Dyes and Pigments,* vol. 140, pp. 480-490, 2017.
[17] Y. Nuhoglu and E. Malkoc, "Thermodynamic and kinetic studies for environmentaly friendly Ni (II) biosorption using waste pomace of olive oil factory," *Bioresource technology,* vol. 100, pp. 2375-2380, 2009.
[18] I. I. Albanio, P. C. L. Muraro, and W. L. da Silva, "Rhodamine B dye adsorption onto biochar from olive biomass waste," *Water, Air, & Soil Pollution,* vol. 232, p. 214, 2021.
[19] T. Somsiripan and C. Sangwichien, "Enhancement of adsorption capacity of Methylene blue, Malachite green, and Rhodamine B onto KOH activated carbon derived from oil palm empty fruit bunches," *Arabian Journal of Chemistry,* vol. 16, p. 105270, 2023.
[20] F. Aguilar, H. Autrup, S. Barlow, L. Castle, R. Crebelli, W. Dekant*, et al.*, "Opinion of the Scientific Panel on Food Additives, Flavourings, Processing Aids and Materials in Contact with Food on a request from the Commission related to an application on the use of cassia gum as a food additive," *EFSA JOURNAL,* vol. 389, pp. 1-16, 2006.
[21] S. Merouani, O. Hamdaoui, F. Saoudi, M. Chiha, and C. Pétrier, "Influence of bicarbonate and carbonate ions on sonochemical degradation of Rhodamine B in aqueous phase," *Journal of hazardous materials,* vol. 175, pp. 593-599, 2010.
[22] R. Mohammed and H. Almashhadani, "Synthesis, characterization and thermodynamic study of a polymer nanocomposite from methyl acrylate and zirconium chloride as an anti-corrosion

coating for carbon steel," *Intnational Journal of Corrosion and Scale Inhibition,* vol. 12, pp. 1180-1191, 2023.
[23] A. Paulraj and A. T. Elizabeth, "Removal of rhodamine B and congo red from aqueous solutions by adsorption onto activated carbons," *Chemical Science Transactions,* vol. 5, pp. 87-96, 2016.
[24] R. T. Salim and D. E. AL-Mammar, "Adsorption of Azo Dye Onto TiO2 Nanoparticles Prepared by a Novel Green Method: Isotherm and Thermodynamic Study," *Iraqi Journal of Science,* vol. 64, pp. 3779-3792, 2023.
[25] A. M. Abbas, Y. I. Mohammed, and T. A. Himdan, "Adsorption kinetic and thermodynamic study of congo red dye on synthetic zeolite and modified synthetic zeolite," *Ibn AL-Haitham Journal For Pure and Applied Science,* vol. 28, pp. 54-72, 2017.
[26] M. Abbas, "Experimental investigation of titanium dioxide as an adsorbent for removal of Congo red from aqueous solution, equilibrium and kinetics modeling," *Journal of Water Reuse and Desalination,* vol. 10, pp. 251-266, 2020.
[27] J. Sahara, A. Naeem, M. Farooq, S. Zareen, and A. Rahman, "Thermodynamic studies of adsorption of rhodamine B and Congo red on graphene oxide," *Desalination and Water Treatment,* vol. 164, pp. 228-239, 2019.
[28] F. A. Hiawi and I. H. Ali, "Study the Interaction Adsorptive Behavior of Sunset Yellow Dye and Loratadine Drug: Kinetics and Thermodynamics Study," *Ibn AL-Haitham Journal For Pure and Applied Sciences,* vol. 36, pp. 186-196, 2023.
[29] K. A. Al-Rudaini, "Adsorption removal of Rhodamine-B dye from aqueous solution using rhamnus stone as low cost adsorbent," *Al-Nahrain Journal of Science,* vol. 20, pp. 32-41, 2017.
[30] A. A. Inyinbor, F. A. Adekola, and G. A. Olatunji, "Adsorption of Rhodamine B dye from aqueous solution on Irvingia gabonensis biomass: kinetics and thermodynamics studies," *South African Journal of Chemistry,* vol. 68, pp. 115-125, 2015.
[31] O. S. Bello and M. A. Ahmad, "Coconut (Cocos nucifera) shell based activated carbon for the removal of malachite green dye from aqueous solutions," *Separation Science and Technology,* vol. 47, pp. 903-912, 2012.
[32] N. A. Khan, K. Saeed, I. Khan, T. Gul, M. Sadiq, A. Uddin*, et al.*, "Efficient photodegradation of orange II dye by nickel oxide nanoparticles and nanoclay supported nickel oxide nanocomposite," *Applied Water Science,* vol. 12, p. 131, 2022.
[33] A. Eskhan, F. Banat, M. Selvaraj, and M. Abu Haija, "Enhanced removal of methyl violet 6B cationic dye from aqueous solutions using calcium alginate hydrogel grafted with poly (styrene-co-maleic anhydride)," *Polymer Bulletin,* vol. 76, pp. 175-203, 2019.
[34] A. Nayak, J. K. Sahoo, S. K. Sahoo, and D. Sahu, "Removal of congo red dye from aqueous solution using zinc oxide nanoparticles synthesised from Ocimum sanctum (Tulsi leaf): a green approach," *International Journal of Environmental Analytical Chemistry,* vol. 102, pp. 7889-7910, 2022.
[35] S. Sonawane, P. Chaudhari, S. Ghodke, S. Phadtare, and S. Meshram, "Ultrasound assisted adsorption of basic dye onto organically modified bentonite (nanoclay)," *Journal of Scientific & Industrail Research,* vol. 68, pp. 162-167, 2009.
[36] J. S. Piccin, L. A. Feris, M. Cooper, and M. Gutterres, "Dye adsorption by leather waste: mechanism diffusion, nature studies, and thermodynamic data," *Journal of Chemical & Engineering Data,* vol. 58, pp. 873-882, 2013.
[37] S. Lairini, K. El Mahtal, Y. Miyah, K. Tanji, S. Guissi, S. Boumchita*, et al.*, "The adsorption of Crystal violet from aqueous solution by using potato peels (Solanum tuberosum): equilibrium and kinetic studies," *Journal of Materials and Environmental Sciences,* vol. 8, pp. 3252-3261, 2017.
[38] G. Ch, "Studies in adsorption. Part XI. A system of classification of solution adsorption isotherms, and its use in diagnosis of adsorption mechanisms and in measurements of specific surface areas of solids," *Journal of the Chemical Society,* vol. 786, pp. 3973-3993, 1960.
[39] Z. A. Najm, M. A. Atiya, and A. K. Hassan, "Biogenesis Synthesis of ZnO NPs: Its adsorption and photocatalytic activity for removal of acid black 210 dye," *Karbala International Journal of Modern Science,* vol. 9, p. 15, 2023.

[40] P. Kaur, P. Bansal, and D. Sud, "Adsorption Behaviour of quinalphos and its leaching potential in different agricultural soils," *Soil and Sediment Contamination: An International Journal,* vol. 30, pp. 730-742, 2021.
[41] R. A. Mahmood and S. S. Mohammed, "Kinetic and thermodynamic study of adsorption of an industrial food dye using Iraqi clay," *Journal of Population Therapeutics and Clinical Pharmacology,* vol. 30, pp. 279-287, 2023.
[42] C. Clavijo and J. F. Osma, "Functionalized leather: A novel and effective hazardous solid waste adsorbent for the removal of the diazo dye congo red from aqueous solution," *Water,* vol. 11, p. 1906, 2019.
[43] A. Dada, A. Olalekan, A. Olatunya, and O. Dada, "Langmuir, Freundlich, Temkin and Dubinin–Radushkevich isotherms studies of equilibrium sorption of Zn2+ unto phosphoric acid modified rice husk," *IOSR Journal of applied chemistry,* vol. 3, pp. 38-45, 2012.
[44] F. Adella and D. Kurniawati, "Adsorption of Rhodamine B from Aqueous Solution Using Langsat (Lansium domesticum) Shell Powder," in *International Conference on Biology, Sciences and Education (ICoBioSE 2019)*, 2020, pp. 273-276.
[45] M. Sureshkumar and C. Namasivayam, "Adsorption behavior of Direct Red 12B and Rhodamine B from water onto surfactant-modified coconut coir pith," *Colloids and Surfaces A: Physicochemical and Engineering Aspects,* vol. 317, pp. 277-283, 2008.
[46] S.-H. Chang, K.-S. Wang, H.-C. Li, M.-Y. Wey, and J.-D. Chou, "Enhancement of Rhodamine B removal by low-cost fly ash sorption with Fenton pre-oxidation," *Journal of hazardous materials,* vol. 172, pp. 1131-1136, 2009.
[47] Y. Zhao, H. Yang, J. Sun, Y. Zhang, and S. Xia, "Enhanced adsorption of rhodamine B on modified oil-based drill cutting ash: characterization, adsorption kinetics, and adsorption isotherm," *ACS omega,* vol. 6, pp. 17086-17094, 2021.
[48] Z. Zhang, I. M. O'Hara, G. A. Kent, and W. O. Doherty, "Comparative study on adsorption of two cationic dyes by milled sugarcane bagasse," *Industrial Crops and Products,* vol. 42, pp. 41-49, 2013.
[49] A. A. Mizhir, H. S. Al-Lami, and A. A. Abdulwahid, "Kinetic, Isotherm, and Thermodynamic Study of Bismarck Brown Dye Adsorption onto Graphene Oxide and Graphene Oxide-Grafted-Poly (n-butyl methacrylate-co-methacrylic Acid)," *Baghdad Science Journal,* vol. 19, pp. 0132-0132, 2022.
[50] N. Laskar and U. Kumar, "Adsorption of Safranin (Cationic) dye from water by Bambusa tulda: Characterization and ANN modeling," *Environmental Engineering Science,* vol. 35, pp. 1361-1375, 2018.
[51] F. F. Mohammed, "Equilibrium, Kinetic, and Thermodynamic Study of Removing Methyl Orange Dye from Aqueous Solution Using Zizphus spina-christi Leaf Powder," *Baghdad Science Journal,* vol. 20, pp. 0296-0296, 2023.
[52] S. H. Kareem and A. Enaas, "Adsorption of Congo, Red Rhodamine B and Disperse blue dyes from aqueous solution onto raw flint clay," *Baghdad Science Journal,* vol. 9, pp. 680-688, 2012.